J Mater Sci (2007) 42:5497–5507
DOI 10.1007/s10853-006-0989-4

On the solid-state ageing behaviour of the polysaccharide, guar gum

L. L. Barré · A. S. Vaughan · S. J. Sutton

Received: 1 September 2006 / Accepted: 21 September 2006 / Published online: 3 April 2007

Abstract Dilute solution viscometry was used to explore the effect of solid-state ageing on the interactions that occur between guar gum and water. The resulting data set, derived from nearly 700 independent experiments, led to a value for the Flory–Huggins interaction parameter, χ, of 0.56 ± 0.12. This value, which appeared independent of ageing, is in good agreement with the majority of published data. The effect of ageing on molar mass was also explored, using Mark–Houwink–Sakurada (MHS) theory. Absolute molar mass values were found to depend sensitively on the choice of MHS constants, but the effect of ageing was unequivocal; under all conditions, it resulted in a pronounced decrease in molar mass. In concert, these results strongly suggest that, in guar, solid-state ageing reactions are largely associated with scission of the molecular backbone. This hypothesis was then tested by infra-red and Raman spectroscopy. Although infra-red spectroscopy did reveal some subtle differences between the spectra of guar and locust bean gum (LBG), a related polysaccharides with a different galactose:mannose ratio, no equivalent effects were seen in aged guar. However, clear differences between the Raman spectra of guar and LBG were seen, demonstrating that the technique is well capable of revealing changes in galactose:mannose ratios. Examination of aged guar samples revealed no comparable effects, reinforcing the notion that, in this polysaccharide, chain scission reactions dominate such that solid-state ageing does not lead to changes in the nature of its interaction with water.

L. L. Barré · A. S. Vaughan (✉)
School of Electronics and Computer Science, University of Southampton, Highfield, Southampton SO17 1BJ, UK
e-mail: asv@ecs.soton.ac.uk

S. J. Sutton
National Grid, NGT House, Warwick Technology Park, Gallows Hill, Warwick, Coventry CV34 6DA, UK

Introduction

The galactomannans constitute a family of water-soluble polysaccharides that function as food reserves within certain plants [1–3]. These polymers consist, principally, of a 1,4-linked β-D-mannopyranosyl backbone (mannose units), with pendent 1,6-linked α-D-galactopyranosyl substituents (galactose units) [1, 4]. The family of materials includes guar gum, locust bean gum, tara gum and fenugreek gum, which differ from one another in terms of both their galactose: mannose ratios [1–5] and the way in which the galactose is distributed along the molecular backbone (ordered, random or as blocks) [2, 3]. In terms of industrial consumption, guar (galactomannan-1, 2) is the most important of these polysaccharides [4]. The distribution of pendent galactose groups along the molecular backbone results in it interacting strongly with water, which leads to many potential application areas; the molecular structure of this polymer is shown schematically in Fig. 1. In the food industry, for example, the thickening properties of guar at low concentrations are widely exploited [6–11]. These same characteristics are also employed in the textile and paper industries [4], and when guar is added to drilling fluids [1] or used in hydraulic fracturing processes [6].

Where guar is used simply to provide an immediate thickening effect, its stability is not an issue of great concern. However, when it is used in a chemically active environment, degradation is of considerable interest [6, 12]; in the pharmaceutical industry, for example, guar has

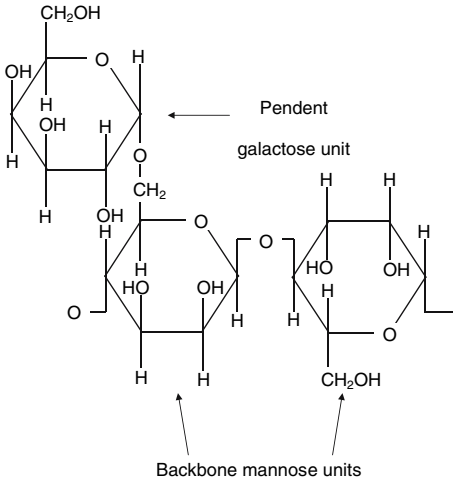

Fig. 1 Schematic diagram showing the molecular structure of guar, which comprises, on average, approximately one pendent galactose unit to every two backbone mannose units. Figure derived from reference 5

been considered for use as an excipient, with the objective of controlling drug-release within the body [13]. Equally, issues of stability and degradation will also relate to any application in which the properties of guar are exploited over prolonged timescales; for example, as part of a protection system in high value plant that is required to perform reliably for a period of several decades.

In high voltage power cables, traditional paper/oil insulation systems have now been largely superseded by polymeric insulation, notably, polyethylene. However, following their widespread introduction in the early 1960s, many polyethylene-insulated cables began to fail through a process termed water-treeing [14]. In this, water diffuses through the hydrophobic polymeric insulation and accumulates at sites of impurities to form water filled cavities [15] which, under the action of the local electric field, grow and develop a tree-like form [16]. Ultimately, the growth of these structures results in catastrophic breakdown of the insulation. The engineering solution that was initially devised to counter this involved the extrusion of a continuous metallic sheath (~1 mm in thickness) around the core of the cable, such that under normal operating conditions, water is unable to reach the insulation. Although this is an effective means of providing a permanent water barrier with considerable mechanical integrity, it is also costly and, necessarily, gives rise to extremely bulky and inflexible cables. An alternative is to replace the traditional metallic sheath with a lightweight and flexible aluminium foil. While this would provide an effective water barrier, so long as it remained intact, it would not possess the same mechanical integrity as conventional designs, leaving the cable susceptible to water ingress via any punctures suffered during installation or in subsequent service.

As described above, much of the practical importance of guar stems from its strong interactions with water. Consequently, a novel application that has been proposed for this polysaccharide is as a water-trapping medium within the aluminium foil sheath of lightweight power cable designs. In the event of puncture, the guar would then act as secondary protection, absorbing any water that penetrated the primary metallic barrier and, thereby, preventing the water from diffusing throughout the structure. However, power cables are designed to operate for 40 years with core temperatures up to 90 °C. Consequently, the stability of the guar and, in particular, the constancy of its interactions with water are of critical importance to this novel design concept.

In this investigation we therefore set out to examine the solid-state thermal stability of a technological guar system. Although the short-term thermal degradation of galactomannans has been studied in aqueous solutions and suspensions, where hydrolysis reactions are likely to dominate [5, 6, 9], we are not aware of any previous work involving solid state ageing and relatively long times (of the order of months). Our specific objectives in this work were:

(i) To determine the fundamental nature of the interactions that occur between water and a guar system proposed for power cable use; reported values of the guar/water interaction parameter, range from 0.2 to 0.8 [8, 17, 18].
(ii) To examine the effect of different ageing conditions on subsequent guar/water interactions, with a view to understanding the long-term behaviour of this polysaccharide when used as a water blocking system within a power cable.
(iii) To explore, spectroscopically, consequent molecular changes and to relate these to changes in the interactions between guar and water that occur on ageing.

Experimental

Sample ageing

The guar gum used in this work was provided by National Grid; this material is an unrefined commercial grade for use in power cable applications. Ageing of dry guar powders was performed in both a dry nitrogen atmosphere (to simulate ageing within a sealed cable) and in air (to promote oxidation and hydrolysis reactions—as might occur after puncture of the sheath). Ageing for 3, 6, 12 and 24 weeks at the technologically relevant temperatures of 50 and 90 °C was performed, to give a total of 16 differently aged samples plus an unaged reference. Throughout this paper, specific samples are referred to using a

nomenclature that defines, in turn, the material, the ageing temperature, the atmosphere and the ageing time in weeks. Thus, G90/N/24 indicates a specific sample of guar that had been aged at 90 °C in dry nitrogen for a period of 24 weeks. A similar notation is used where we wish to refer to the global data set obtained from a group of samples. For example, all the samples that had been aged at 90 °C in air are, collectively, indicated by G90/A.

Preparation of guar solutions

To prepare specimens for dilute solution viscometry, 1 g of the appropriate guar specimen was precisely weighed out with a Sartorius MC210P microbalance, added to 250 mL of distilled-deionized water (DDW) and left to hydrate. From the work of Chen et al. [19], the characteristic swelling time, τ, of a non-porous hydrogel can be written:

$$\tau = L^2/D \quad (1)$$

where L represents the characteristic dimension of the constituent particles and D is a diffusion coefficient. From optical microscopy, the typical size of the guar particles in our sample is of the order of 1 mm and, therefore, the above equation predicts that these should become entirely swollen in about one day, assuming a value of 10^{-7} cm^2 s^{-1} for D [19]. The relationships between hydration time (defined as, $t_{0.8}$, the duration required for the viscosity of the system to reach 80% of its maximum value), initial concentration and molar mass have also been studied experimentally for a commercial guar system; that is, a similar material to the one used here. This work reported $t_{0.8}$ to be of the order of 3 h for a concentration of 0.4% guar, when hydrated using a specific mixing device [20]. Using the same methodology, we explored the hydration characteristics of our material by performing sequential viscometric experiments after different hydration times. Measurements of the efflux time of these fresh guar solutions demonstrated that this parameter reaches a maximum after about 24 h of hydration at room temperature, which is consistent with the studies described above [19, 20]. Nevertheless, to ensure maximum hydration, our samples were routinely left to hydrate for 100 h at room temperature, before being refined.

Raw guar can contain a range of components, including cell debris, crude fibres, ashes and proteins [3, 5, 6, 11, 17, 20] and, as a result, a number of refining procedures have been employed by different workers to separate the water-soluble polysaccharide molecules from such insoluble constituents. These range from simple ''top-taking'' methods [3], which rely on natural precipitation of the insoluble elements, to sophisticated procedures that aim to obtain highly refined, almost monodisperse samples [7]. However, many refining procedures for polysaccharides rely on centrifugation [6–8, 21, 22] and, consequently, such a procedure was adopted here. Following hydration, a BB VVV centrifuge was used to separate the supernatant solution from the residual suspended gel; after centrifugation, the insoluble components of the guar take the form of a white pellet at the bottom of the vial, so permitting easy separation of the two phases. Pelleting conditions were optimized by exploring the effect of centrifuge speed and time on pellet formation. From these experiments, standard conditions corresponding to a centrifugal force of about 750 g for 15 min were identified. Similar guar refining conditions (700 g for 10 min) have previously been reported by Casas et al. [21].

Dilute solution viscometry

In line with many previous studies [3, 7, 9, 17, 18, 20], an Ubbelohde viscometer was used, in conjunction with a precision Techne water bath, to study the flow characteristics of our guar solutions. A potential problem with this approach concerns non-Newtonian behaviour, since guar is known to exhibit shear thinning [6, 7, 10, 21]. The data of Robinson et al. [10] indicate that shear thinning occurs at a shear rate of ~0.1 s^{-1} at a concentration of 2%, while both Cheng and Prud'homme [6] and Wientjes et al. [7] have reported the onset of shear thinning at ~1 s^{-1} for a 0.5% guar/water system. The effect of concentration on non-Newtonian behaviour has also been explored in a number of other biopolymer/solvent systems and these studies conclude that shear thinning becomes increasingly insignificant [23–25], and can disappear completely [26, 27], as the polymer concentration is reduced. All the data used in this study were therefore obtained below the threshold concentration, C^*, which represents the transition between the dilute and the semi-dilute regime [10]; this is also reported to correspond to the onset of shear thinning [27]. However, with sensitive measurements of this type, contamination and impurities are also potential sources of irreproducibility and, consequently, a number of strategies were employed to explore the impact of such factors on our results. For example, ionic impurities were deliberately added to the solutions to explore their effect [28]; extreme cleaning routines, based upon permanganic acid and hydrogen peroxide [29] were used to remove any organic residues from the viscometer; repeat measurements were routinely made to ensure reproducibility.

After these preliminary studies, the viscosity of each specimen was determined as a function of concentration, through a process of repeated dilution of the refined stock solutions prepared as described above. Eight concentrations were typically used to characterize each system and

each stock solution was tested at five temperatures, namely 27.5, 35, 42.5, 50 and 57.5 °C; the unaged reference material was, additionally, tested at 20 and 65 °C. Thus, the flow behaviour of materials aged under seventeen different ageing conditions was considered as a function of concentration at, at least, five different temperatures. This equates to nearly seven hundred independent viscometry measurements. Subsequent data analysis was ultimately performed using SigmaPlot 2000; the indicated uncertainties correspond to 95% confidence intervals.

Spectroscopy

Spectroscopic data were acquired from a variety of aged guar samples, using standard techniques. Infra-red data were obtained using a Nicolet 710 Fourier transform infra-red (FTIR) instrument; a resolution of 4 cm^{-1} was chosen and, routinely, spectra were acquired by integrating either 128 or 256 spectra. Complementary Raman data were acquired using a Renishaw RM1000 Raman microprobe which, to obtain the data presented here, was operated in its non-confocal mode to maximize the detected signal. Nevertheless, it was still necessary to integrate large numbers of scans (up to 2400 30 s extended scans) to obtain an acceptable spectral quality. Typically, each spectrum therefore took of the order of 24 h to acquire.

Spectral data were also acquired from unaged samples of locust bean gum, galactomannan-1, 4 [4], supplied by TIC Gums. Like guar, LBG is a galactomannan, but whereas guar has one pendant galactose unit for every 1.2–2 backbone mannose units [1–5, 21], in locust bean gum, there is one galactose group for every 3.5–4 mannose units [1–5].

Results

Figure 2 shows the fraction of insoluble material in our various aged systems. From this, it is evident that all of these contain a significant gel fraction and that this varies from specimen to specimen. Daas et al. [3] examined ten different guar grades and visually estimated that all contained 40–60% by mass of insoluble material; quantitative evaluation of the insoluble content was, however, deemed ''to be unreliable'' [3]. Nevertheless, by grouping the data in Fig. 2 in terms of ageing temperature, visual inspection suggests that ageing may reduce the insoluble fraction, with the implication that chain scission reactions are occurring. However, using quantitative criteria, the trends lines in Fig. 2 are not statistically significant.

Dilute solution viscometry is widely used to study the behaviour of macromolecules in solution under conditions

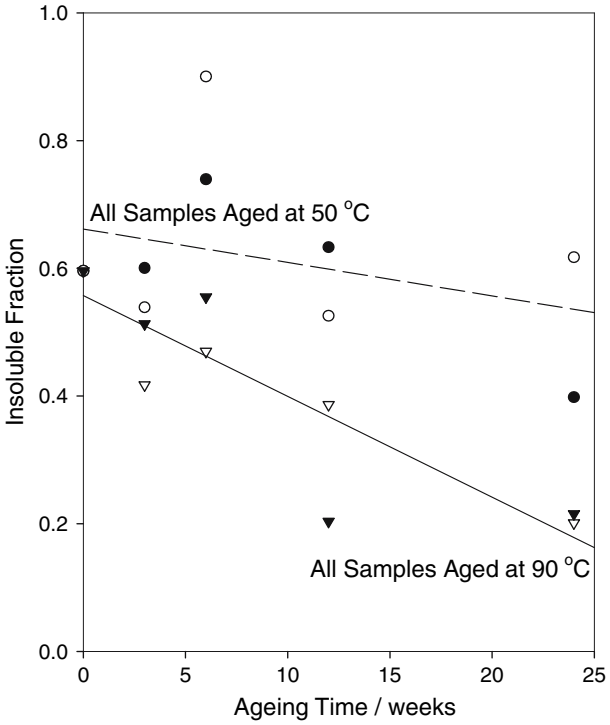

Fig. 2 Plots showing the insoluble fraction in guar samples aged for different times: ● G50/N; ◯ G50/A; ▼ G90/N; ▽ G90/A. The dashed line represents the best fit to all the data obtained from samples aged at 50 °C, while the solid line represents the best fit to all the data obtained from samples aged at 90 °C

of dilute, Newtonian flow. The analysis methodologies reported in the literature are still those originally developed by Huggins [30–32] and by Kraemer [33]; the Huggins equation and the Kraemer equation are, respectively, written:

$$(\eta_{rel} - 1)/C = [\eta] + k'[\eta]^2 C \quad (2)$$

$$\ln(\eta_{rel})/C = [\eta] + k''[\eta]^2 C \quad (3)$$

where η_{rel} represent the relative viscosity, C the solution concentration, $[\eta]$ the intrinsic viscosity, k'' the Kraemer constant and k' the Huggins constant, the physical interpretation of which is the Flory Huggins interaction parameter, χ. The Huggins and Kraemer constant are linked such that [34, 35]:

$$\chi = 0.5 + k'' \quad (4)$$

Here, the Kraemer method was chosen [35] to obtain values for the intrinsic viscosity and the interaction parameter between water and guar, as a function of ageing; the Huggins method was, however, also applied to a subset of data and equivalent results were obtained.

Intrinsic viscosity and molar mass

Figure 3 shows the dependence of the intrinsic viscosity, $[\eta]$, on flow temperature for the unaged reference system and our four differently aged sets of guar samples (G50/N/3; G50/A/3; G90/N/3; G90/A/3). When presented in this way, it is evident that this parameter is markedly influenced by ageing, but that changing the temperature of the flow experiment within this relatively narrow range does not result in any systematic variation in $[\eta]$; the same conclusion is reported elsewhere for the polysaccharide xanthan [36]. Thus, the data used to generate Figure 3 were grouped to derive a mean values for $[\eta]$ for each aged guar sample (together with related uncertainties).

The resulting values of $[\eta]$ were then analyzed using conventional Mark-Houwink-Sakurada (MHS) equation, in line with many previous studies [1, 7, 9, 10, 18, 22]. That is:

$$[\eta] = K\overline{M}^{a} \tag{5}$$

where $\overline{M}$ represents an average molar mass and K and a are constants that relate to the specific solute/solvent combination. However, published values for K and a for the guar/water system vary significantly. For example, Wientjes et al. [7] derived values of $K = (6.7 \pm 1.1) \times 10^{-2}$ ml g^{-1} and $a = 1.05 \pm 0.01$ by relating rheological measurements to molar masses obtained by gel permeation chromatography (GPC). This work has the merit of having used highly refined, narrow fractions of guar (polydispersity values as low as 1.02 are reported) but, on theoretical grounds, this value for a does appear rather large [18, 37]. In contrast, Beer et al. derived values of $K = 5.13 \times 10^{-2}$ ml g^{-1} and $a = 0.72$ [22], which are consistent with earlier measurements [10]. Since our choice of K and a will impact significantly on the absolute molar mass values we obtain, some independent method of selecting these is therefore desirable.

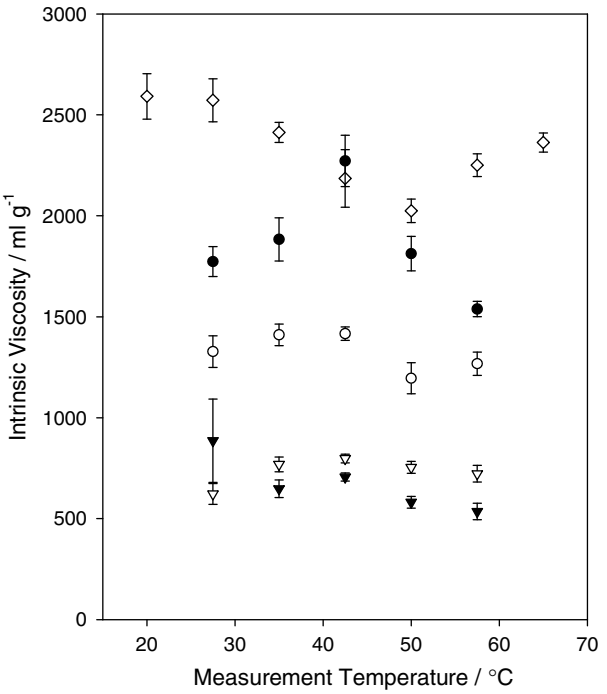

Fig. 3 Typical plots showing the effect of measurement temperature on the intrinsic viscosity, obtained from an unaged reference specimen plus guar samples aged for three weeks under different conditions: ◇ unaged reference material; ● G50/N/3; ◯ G50/A/3; ▼ G90/N/3; ∇ G90/A/3

Tayal and Khan [38] reported on three cleavage models for guar, which they subsequently employed numerically to analyze chain scission induced by both sonication and enzymatic hydrolysis. These involved random scission, central scission or chain scission based upon a Gaussian probability distribution. Nevertheless, most studies [1, 6, 9, 18, 39] have assumed that degradation reactions in polysaccharides follow pseudo first order kinetics, which can be expressed as [6]:

$$\frac{1}{\overline{M}_t} - \frac{1}{\overline{M}_0} = \frac{k_s}{m}t \tag{6}$$

where $\overline{M}_0$ is the initial molar mass, $\overline{M}_t$ is the molar mass after a degradation time t, m is the molar mass of the repeat unit and k_s is the rate constant for chain scission. Substituting from Eq. 5 into Eq. 6 leads to an expression of the form [9]:

$$\frac{1}{[\eta]_t} = (A + Bt)^{a} \tag{7}$$

where

$$A = \frac{1}{[\eta]_0^{1/a}} \tag{8}$$

$$B = \frac{k_s}{mK^{1/a}} \tag{9}$$

$[\eta]_t$ is the intrinsic viscosity after ageing for a time t and $[\eta]_0$ is the intrinsic viscosity of the unaged reference.

Particularly for the case where a is close to 1, Eq. 7 can easily be solved numerically to provide values for A and B, provided suitable data sets exist. In the case of our data, we have four independent ageing conditions, which will be governed by different rate constants (k_s and, therefore B values). However, depending upon the precise chemistry involved in the degradation process, it is possible that all four data sets could share a common A value. Specifically, this requires that the mechanism of degradation in each case serves to modify the molecular hydrodynamic volume

solely as a result of changes in molecular length, not through changes in polymer/solvent interaction energetics. To test this hypothesis, intrinsic viscosity was plotted against ageing time for our four different ageing conditions and the data were fitted to Eq. 7. As reported elsewhere [1], our experimental data do not conform to Eq. 6 at the extremes of ageing and, therefore, samples aged for 24 weeks and that represented in Fig. 4 by the data point shown in grey (G90/A/12) were omitted from this process. Figure 4 shows the resulting optimized, self consistent plots of intrinsic viscosity against ageing time; the best fit lines shown were generated using values of $[\eta]_0 = 2353$ mL g^{-1} (compared with the experimental value of 2343 ± 190 mL g^{-1}) and $a = 0.77$. This value for a lies close to the upper limit for a random coil structure [10, 17], which is reasonable given that guar is considered to be a stiffened polysaccharide [10, 27]. From Eq. 9, B contains both K and k_s and, therefore, it is not possible to derive an independent value for the MHS K parameter in this way, using just four data sets. Nevertheless, in view of our derived value for a, we chose to use the values for K and a reported by Beer et al. [22] for the analysis that follows.

Figure 5 shows the variation of molar mass of guar with ageing, from which it can be seen that $\overline{M}_t$ falls approximately exponentially with ageing time from an initial molar mass of $(3.0 \pm 0.2) \times 10^6$ g mol^{-1}. In contrast, Cheng et al. [17], Beer et al. [22] and Kök et al. [1], respectively, reported values of 1.9×10^6, 1.6×10^6 and 1.1×10^6 g mol^{-1} for the molar mass of virgin guar, based upon GPC results; Simonet et al. [8] used small angle light scattering to derive a value for the mass average molar mass, $\overline{M}_w$, of 2.17×10^6 g mol^{-1}. Although our estimate of 3.0×10^6 g mol^{-1} therefore appears rather high, the absolute significance of this discrepancy is difficult to evaluate, for a number of reasons.

(i) Guar is a natural product, and Wang et al. [20] have described commercial guar gum flours with molar masses up to 2.82×10^6 g mol^{-1}.
(ii) Polydispersity has been shown to be critical in terms of the evaluation of K and a [22]; our material is an unrefined commercial system, whereas the polymers used to evaluate these parameters have generally corresponded to relatively narrow fractions.
(iii) Our use of the MHS equation depends critically upon the chosen values of K and a. Repeating the above analysis with $K = 6.7 \times 10^{-4}$ mL g^{-1} and $a = 1.05$, as derived by Wientjes et al. [7], leads to a value of $(1.71 \pm 0.10) \times 10^6$ g mol^{-1} for the molar mass of our virgin guar, in good agreement with the majority of values quoted above.

While our choice of MHS parameters is clearly important in terms of the absolute molar mass values we obtain, it does however, do nothing to affect the form of the data

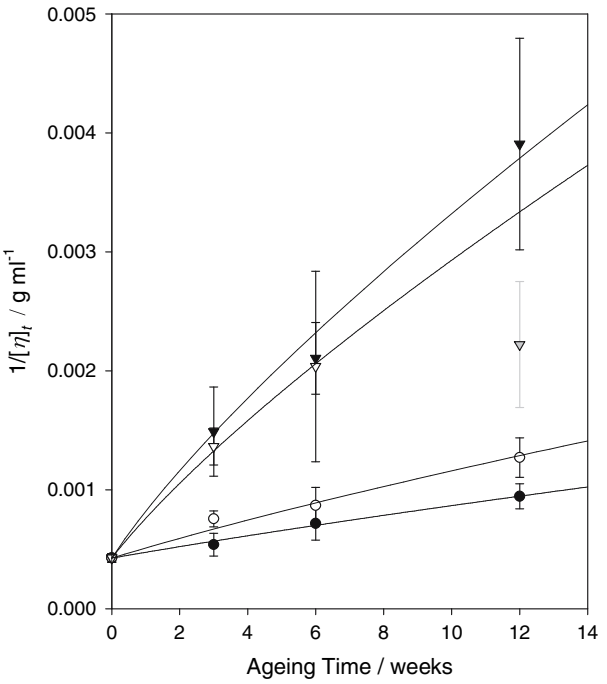

Fig. 4 Variation of intrinsic viscosity with ageing time; the solid lines correspond to self consistent best fit lines generated using values of $[\eta]_0 = 2353$ ml g^{-1} and $a = 0.77$: ● G50/N; ◯ G50/A; ▼ G90/N; ▽ G90/A

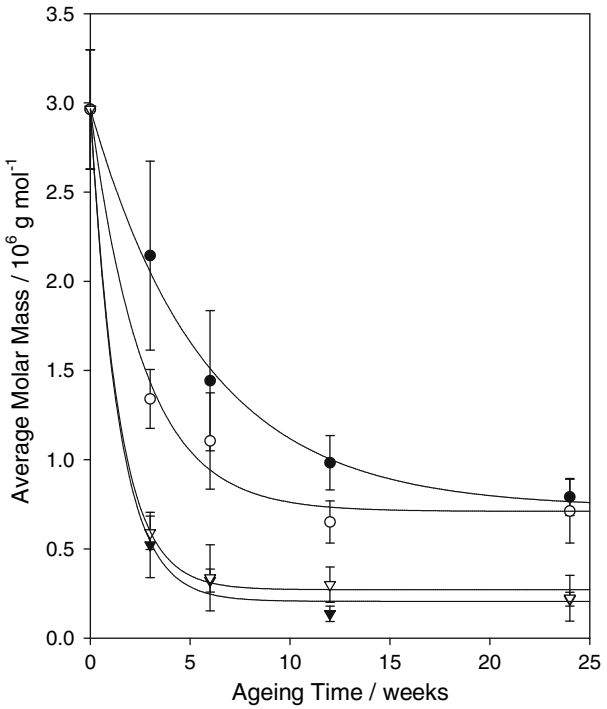

Fig. 5 Variation of average molar mass with ageing time for guar samples aged under different conditions: ● G50/N; ◯ G50/A; ▼ G90/N; ▽ G90/A

shown in Fig. 5; our objective here was to examine molecular *changes* induced by solid state ageing, rather to obtain an absolute molar mass value for our particular initial guar sample. From Fig. 5, the molar mass of guar clearly drops significantly during solid state ageing under all four sets of imposed conditions.

Effect of ageing on the interactions between guar and water

From the preceding section, it is evident that the molecular backbone of guar is extremely sensitive to scission processes when the material is aged at 50 or 90 °C. When considering the effect of ageing on guar/water interactions, two broad scenarios can therefore be envisaged.

(i) Chain scission is accompanied by appreciable reactions involving the pendent galactose units. Since the interactions of guar and related polysaccharides with water are intimately linked to steric hindrance associated with the distribution of galactose groups along the molecular backbone, if such reactions were to occur, then ageing should result in significant changes in the interaction parameter, χ.
(ii) Alternatively, reactions are confined to the molecular backbone, whereupon, ageing will result in reductions in molar mass, as described above, but no appreciable change in χ.

Values of χ were therefore calculated from our experimental data using Eq. 4. As in the case of $[\eta]$ above, 87 independent estimates for χ were obtained in this way, each corresponding to a unique combination of ageing and flow conditions. Consider, first, the effect of flow temperature on χ where, according to Hamley [40], a hyperbolic relation between χ and T exists for some systems. That is:

$$\chi = K_1 + \frac{K_2}{T} \tag{10}$$

where K_1 and K_2 are constants. However, our data, are not well described by this model, suggesting that either this relationship is inappropriate here or that, for the guar/water system, the value of K_2 is sufficiently small, compared with experimental uncertainty, that the resultant variation in χ is insignificant within the relatively small temperature range considered here. By assuming that χ is effectively independent of flow temperature, our data were then grouped to give an average value of χ for each of our 17 differently aged samples. No trends emerged. This process was repeated for all combinations of factors, with the same conclusion. We therefore believe that there is little to differentiate the χ values derived from our various samples, with the implication that our 87 individual values for χ are, in reality, equivalent. Consequently, standard statistical procedures were applied [41] to the resulting large data set, which leads to a value for χ of 0.56 ± 0.12 that is independent of ageing. Although, classically, $\chi = 0.5$ corresponds to θ-solvency, the literature suggests that for a good solvent, χ falls in the range 0.25–0.40 while, for theta solvents, values in the range 0.5–0.7 would be anticipated [17, 18, 34, 35]. Consequently, we conclude that our value of $\chi = 0.56 \pm 0.12$ indicates that strong interactions occur between guar and water and that, despite changes in molar mass, these are not markedly affected by ageing under conditions relevant to cable technology.

Before moving on it is, however, appropriate to compare the above value for the guar/water interaction parameter with those previously reported in the literature. Cheng et al. reported that, for the guar/water system, χ lies in the range 0.7–0.8 for unaged polymer [17, 18]. However, following enzymatic hydrolysis, this value fell to 0.2–0.3 as a result of the reduction in molar mass [18]. These workers related their high initial value of χ to aggregation processes, which only occur when guar molecules are not degraded. Indeed, in the locust bean gum/water system, values of χ in the range 0.8–0.9 have been reported [11] and associated with the presence of hyper-entanglements. That is, intermolecular interactions via extended sequences of unsubstituted mannose residues [42, 43]. Thus, it is possible that the values of Cheng et al. have a similar origin, and may be associated with either the source of the guar or the way in which it was processed. As discussed in the experimental section, considerable care is required to ensure complete guar hydration; Azero et al. [43] derived a χ value of 0.59 for aqueous solution of guar, but indicated that this could be influenced by the chosen centrifugation and filtering procedures. Elsewhere, Wientjes et al. [7] reported on water-guar interactions in guar samples whose molar mass varied by nearly one order of magnitude and derived a molar mass-independent χ value of 0.55 ± 0.05. Simonet et al. [8] derived a value for χ of 0.483 from light scattering data. In conclusion, where appropriate parallels can be drawn, we believe that our value for χ is consistent with the bulk of published data.

FTIR Spectroscopy

While changes in intrinsic viscosity demonstrate that the guar backbone is sensitive to chain scission reactions under the ageing conditions employed here, the above analysis reveals no systematic influence of ageing on χ, with the implication that the galactose : mannose ratio remains unaffected. These conclusions concerning the effect of ageing on the molecular structure of guar are, of course, based entirely upon indirect evidence and, for this reason,

we chose to probe the molecular structure of aged guar directly by spectroscopic means. However, in terms of their constituent function groups, the galactose and mannose units that make up guar are effectively equivalent, as can be seen from Fig. 1; galactose and mannose differ primarily in terms of their conformation. In view of this, and the principal motivation for this study, much of the analysis that follows involves a comparison of guar (nominal galactose : mannose ratio of 1:2) with locust bean gum (LBG) (nominal galactose : mannose ratio of 1:4), a system that interacts much less strongly with water [44–46].

Figure 6 contains spectra obtaining from unaged guar, unaged LBG and a severely aged guar sample that was produced specifically for this spectroscopic study. Before discussing the spectrum obtained from the aged guar, we will first consider FTIR data obtained from unaged reference specimens of guar and LBG. Since we are not aware of any published FTIR analysis of these two polymers, comparisons can only be made with spectral studies of related compounds, such as cellulose [47–49], starches [50] and the monosaccharide α-D-galactose itself [51]. In this way, it is possible to propose matches between reported galactose peaks at 1074 and 1147 cm^{-1} [51] and features in the data shown in Fig. 6a at 1076 cm^{-1} and 1149 cm^{-1}, and to associate the vibrations of starch at 1344 cm^{-1} (COH bending and CH_2 twisting) and 1415 cm^{-1} (CH_2 bending and COO stretching) with some of the overlapping features we see at 1345 cm^{-1} and 1415 cm^{-1}. However, detailed comparison of our FTIR data, in totality, with spectra from the systems listed above leads to few compelling matches. Therefore, we are forced to conclude that, at a detailed level, FTIR spectra of polysaccharides are not simple combinations of the spectra of the monosaccharides of which they are composed. Indeed, Proniewicz et al. [48, 49] have indicated that a single α-anomer of D-glucose will exhibit 18 vibrational modes within the 1200–1500 cm^{-1} region alone, such that it is not possible to identify precisely all the spectral features exhibited by even such a relatively simple structure. Nevertheless, even in the absence of any specific vibrational allocations, by simply treating the data shown in Fig. 6 as characteristic fingerprints, we can qualitatively conclude that the FTIR spectra of guar and LBG are subtly different, for example in the region of 1340 cm^{-1}, as arrowed to the right of Fig. 6b. This therefore implies that major alterations in galactose: mannose ratios do manifest themselves in small, but detectable, changes in the observed FTIR spectra.

Comparing the spectrum of G150/A/0.5 with those obtained from unaged guar and LBG, it is evident that any changes induced by ageing are slight. Specifically, there is no evidence of changes in the region of 1340 cm^{-1}, which could be related to changes in the polymer's galactose: mannose ratio. However, for a sample that had been aged in air at 150 °C, the region around 1730 cm^{-1} is likely to be of particular relevance, since this corresponds to the carbonyl-stretching region. Proniewicz et al. [48] have shown

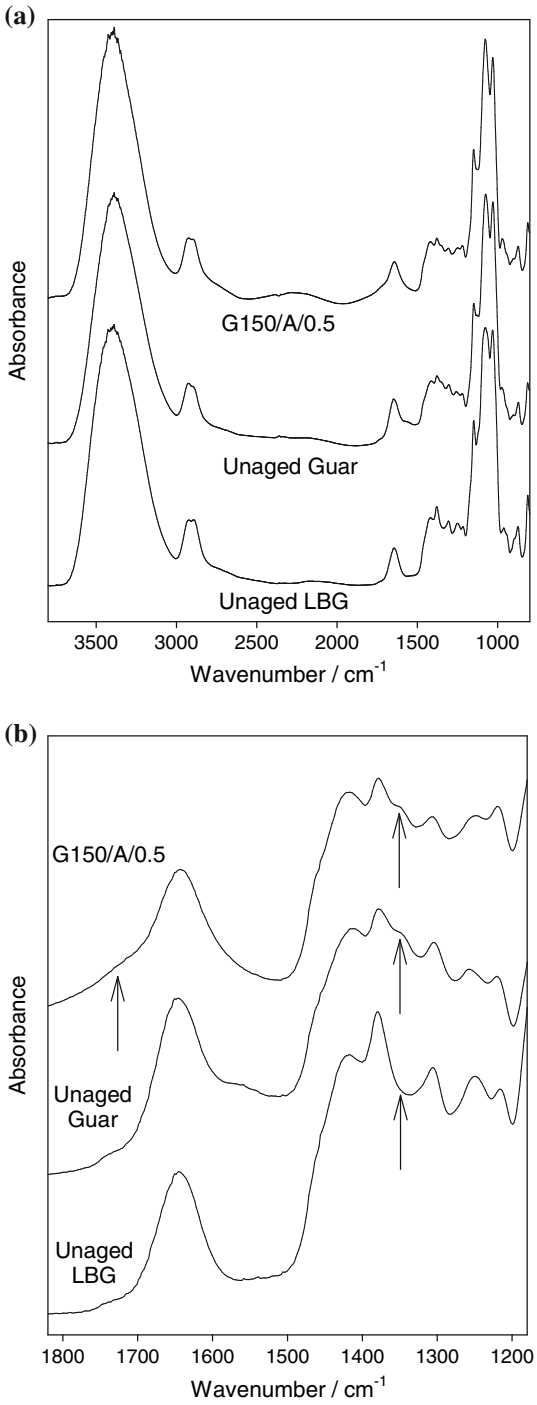

Fig. 6 FTIR spectra comparing unaged locust bean gum and unaged guar (a highly degraded specimen of guar G150/A/0.5 is also included for comparison): (**a**) all three samples appear similar when the complete spectral range is displayed; (**b**) subtle differences between locust bean gum and guar do however exist, such as the feature arrowed at 1350 cm^{-1}

that, in cellulose, ageing results in the formation of a shoulder, which tends to extend the existing 1650 cm^{-1} peak to higher wavenumbers. Some evidence of similar effects can be seen in Fig. 6b (arrowed), implying that ageing guar in air has a similar effect. However, clearly, the magnitude of this is not great, despite the severity of the imposed ageing treatment.

Raman spectroscopy

Raman spectroscopy is a technique that has been shown to be highly sensitive to conformational differences between carbohydrate systems [47, 52–54] and, therefore, it appears an ideal technique with which to probe molecular changes that are perhaps too subtle to be revealed by FTIR. In analyzing Raman data from carbohydrates, two distinct approaches have been adopted in the past. Mrozek et al. [52] acquired Raman spectra from a range of monosaccharide systems, including D-mannose and D-galactose and treated these simply as characteristic fingerprints. In this way, they showed that while spectra obtained from mixtures of two monosaccharides are a linear combination of the Raman spectrum of each component, the behaviour of disaccharides is rather more complex, due to the influence of the glycosidic linkage. Nevertheless, the spectrum of the disaccharide they examined shared sufficient common features with its constituents, that the component monosaccharides could be deduced. The alternative to a fingerprinting approach involves a complete spectral analysis, combining normal mode calculations with the experimental characterization of a range of model systems. However, even then, the strongly coupled nature of the vibrational modes in carbohydrate polymers makes the association of specific spectral features with specific vibrational modes very difficult. Consequently, we will here follow the successful approach of Mrozek et al. [52] and, again, consider our data, simply as spectral fingerprints.

Figure 7 compares Raman spectra obtained from unaged reference samples of guar and LBG. From this figure, it is apparent that changing the galactose: mannose ratio has an appreciable effect on the resultant spectra, since clear differences between guar and LBG can be identified across the range of Raman shifts shown. For example, three peaks are visible in both spectra in the vicinity of 1350 cm^{-1} (left hand arrow). In the LBG spectrum, the central feature at 1343 cm^{-1} is relatively weak, compared with the peak at 1377 cm^{-1} whereas, in the guar spectrum, the 1343 cm^{-1} peak is much more pronounced. The region spanning 800–1000 cm^{-1} (middle arrow) contains a number of features where the intensity again varies between the two spectra. In particular, the feature at 914 cm^{-1} in the spectrum of LBG is strong while that at 823 cm^{-1} is relatively weak; the converse pertains in the guar spectrum. Relative to the peak

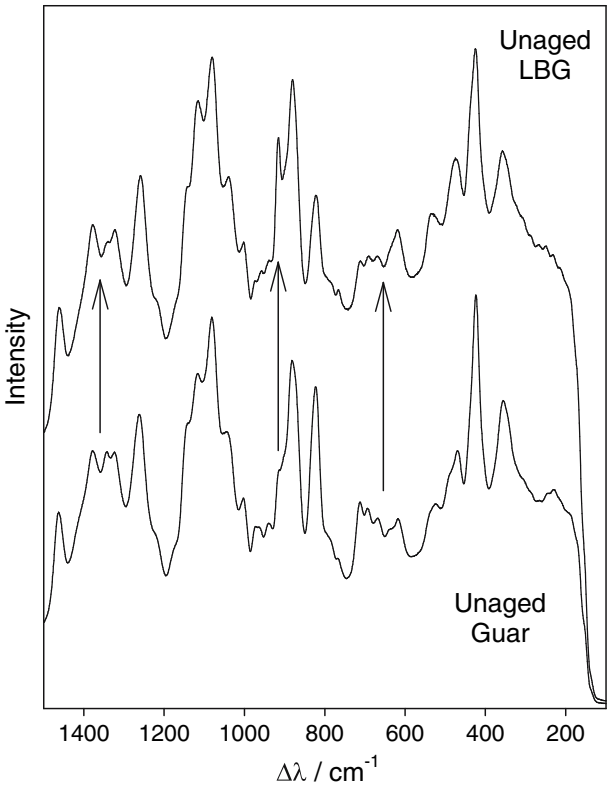

Fig. 7 Raman spectra comparing unaged locust bean gum and unaged guar; significant differences between locust bean gum and guar exist throughout this region of the spectrum and regions of particular significance are arrowed

at 939 cm^{-1}, the small feature located at 972 cm^{-1} is much more prominent in guar than in LBG. Similar variations in the intensity of minor features can be seen around 650 cm^{-1} (right hand arrow). Since LBG and guar differ only in the increased number of pendant galactose groups, it is therefore tempting to associate galactose with those peaks in the guar spectrum that exhibit an increased intensity (e.g. 712, 823, 972 and 1443 cm^{-1}) and to relate those that are more prominent in LBG to mannose (e.g. 618 and 914 cm^{-1}).

Mrozek et al. [52] observed a specific vibration of D-mannose at 904 cm^{-1} whereas nothing was seen in the spectrum of D-galactose in this region; the normal mode analysis of Zhbankov et al. [51] indicated the presence of a Raman active vibrational mode of D-galactose at 978 cm^{-1}. Otherwise, neither experimental nor theoretical data for D-galactose and D-mannose [51, 52] provide any evidence in support of the above assertions; the spectra of such monosaccharides simply contain too many features, even when the complicating effect of the glycosidic linkages are removed. Nevertheless, although specific peak assignments are difficult, the empirical differences between the spectra of guar and LBG shown in Fig. 7 demonstrate that Raman spectroscopy is able clearly to differentiate between polymers that contain different galactose : mannose ratios.

The effect of aging on the Raman response of guar is illustrated in Fig. 8; this compares the Raman spectrum of unaged guar with data obtained from G90/A/24 and G90/N/24, the two most severely aged samples for which fluorescence did not totally dominate. From such data, it is evident that the major effect of ageing is, nevertheless, an increase in fluorescence (vertical offset and sloping background) since all the spectra shown are, otherwise, extremely similar. In particular, the location and relative magnitude of the key markers identified above are entirely equivalent in the aged and reference samples (see Fig. 8b). As in the case of the FTIR results, Raman again demonstrates that while no significant spectral changes result from ageing guar, this is not because the technique is unable to differentiate between systems containing different galactose : mannose ratios. Evidently, Raman is well able to differentiate between guar and LBG.

Conclusions

The effect of solid-state ageing on the molecular structure of guar and the interactions that occur between this polysaccharide and water have been studied by a combination of dilute solution viscometry and vibrational spectroscopy. From the flow behaviour, we conclude that ageing under all the conditions considered here results in an approximately exponential reduction in the molar mass of the polymer with ageing time, such that it asymptotically approaches a value that is dependent upon the imposed ageing temperature. As would be anticipated, chain scission occurs more rapidly at 90 °C than at 50 °C and, at least at the latter temperature, the reaction is accelerated in the presence of oxygen. Despite these changes to the molecular backbone of guar, the guar : water interaction parameter does not vary systematically with any of the imposed experimental conditions (flow temperature, ageing temperature, ageing time, atmosphere), suggesting that solid-sate ageing does not affect the number of pendent galactose groups along the mannose chain. Comparison of guar and the related galactomannan locust bean gum indicates that changing the galactose : mannose ratio results in changes in the observed FTIR spectra, but that these are small. No comparable variations were seen in the spectra of aged guar. The Raman spectra of guar and locust bean gum were found to be significantly different, indicating that this technique is considerably more sensitive to small changes in the molecular structure of polymeric carbohydrates. Despite this, the Raman spectra of aged and unaged guar were again found to be equivalent, except for an increased level of background fluorescence in the latter specimens. When data derived from these three techniques (dilute solution viscometry, FTIR spectroscopy and Raman spectroscopy) are considered in concert, an entirely consistent picture of the effect of solid-state ageing emerges. Ageing results in main chain scission but no significant loss of pendant galactose groups, such that the interactions between aged guar and water are unaffected. Technologically, this indi-

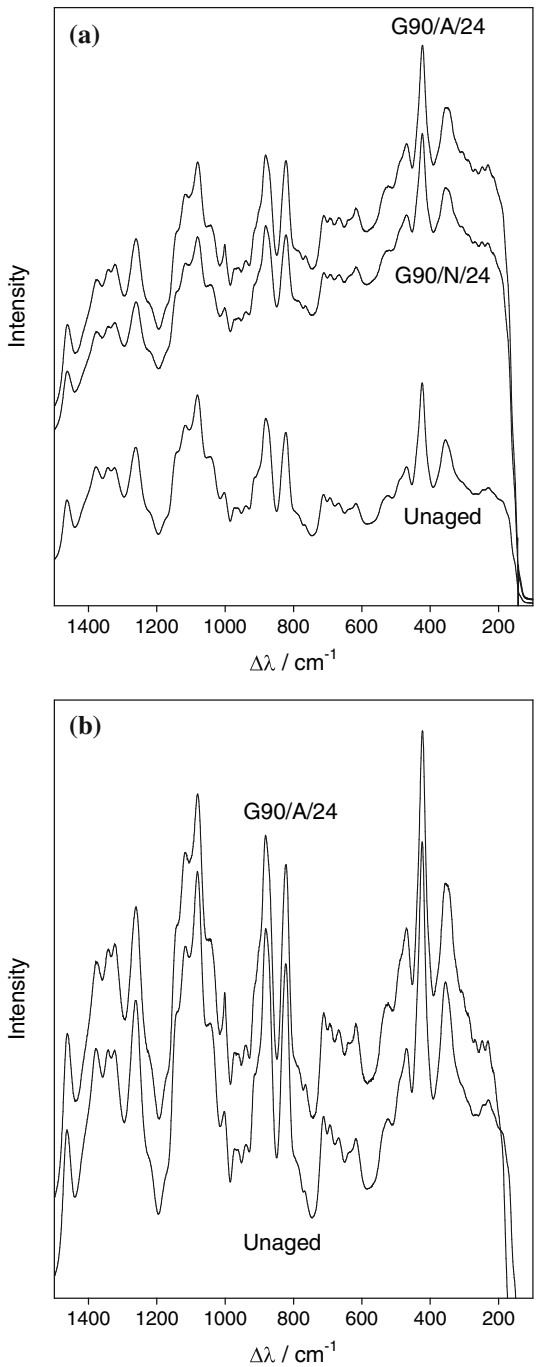

Fig. 8 Raman spectra obtained from an aged and unaged specimens of guar. In (**a**) raw data derived from an unaged specimen are compared with spectra obtained from samples aged for 24 weeks at 90 °C in nitrogen (G/90/N/24) and in air (G/90/A/24) while in (**b**) the unaged sample and G/90/A/24 are compared after removal of the background fluorescence

cates that guar constitutes a suitable water-blocking medium for power cable applications, where strong interactions with water are critical, and need to be retained over a period of time extending to several decades. Although guar does age, this does not occur in a manner that is detrimental to the fundamental function for which it is employed.

Acknowledgements The authors wish to acknowledge the support of National Grid and their permission to publish this work.

References

1. Kök MS, Hill SE, Mitchell JR (1999) Food Hydrocolloids 13:535
2. Daas PJH, Schols HA, De Jongh HHJ (2000) Carbohyd Res 329:609
3. Daas PJH, Grolle K, Van Vliet T, Schols HA, De Jongh HHJ (2002) J Agric Food Chem 50:4282
4. Bayerlein F (1993) In: Meuser F, Manners DJ, Seibel W (eds) Plant polymeric carbohydrates. Royal Society of Chemistry, Cambridge, p 191
5. Garti N, Leser ME (2001) Polym Adv Technol 12:123
6. Cheng Y, Prud'homme RK (2000) Biomacromolecules 1:782
7. Wientjes RHW, Duits MHG, Jongschaap RJJ, Mellema J (2000) Macromolecules 33:9594
8. Simonet F, Garnier C, Doublier J-L (2002) Carbohyd Polym 47:313
9. Lai VM-F, Lii C-Y, Hung W-L, Lu T-J (2000) Food Chem 68:319
10. Robinson G, Ross-Murphy SB, Morris ER (1982) Carbohyd Research 107:17
11. Fernandes PB (1995) J Food Eng 24:269
12. Ferguson MJ, Jones GP (2000) J Sci Food Agric 80:166
13. Vandamme TF, Lenourry A, Charrueau C, Chaumeil J-C (2002) Carbohyd Polym 48:219
14. Shaw MT, Shaw SH (1984) IEEE Trans Electr Insul 19:419
15. Johnson GE, Bair HE, Matsuoka S, Anderson EW, Scott JE (1980) In: Rowland SP (eds) Water in Polymers. ACS, Washington DC, p 451
16. Moreau E, Mayoux C, Laurent C, Boudet A (1993) IEEE Trans Electr Insul 28:54
17. Cheng Y, Brown KM, Prud'homme RK (2002) Biomacromolecules 3:456
18. Cheng Y, Brown KM, Prud'homme RK (2002) Int J Biol Macromol 31:29
19. Chen J, Park H, Park K (1999) J Biomed Mater Res 44:53
20. Wang Q, Ellis PR, Ross-Murphy SB (2003) Carbohyd Polym 53:75
21. Casas JA, Mohedano AF, Garcia-Ochoa F (2000) J Sci Food Agric 80:1722
22. Beer MU, Wood PJ, Weisz J (1999) Carbohyd Polym 39:377
23. Ndjouenkeu R, Goycoolea FM, Morris ER, Akingbala JO (1996) Carbohyd Polym 29:263
24. Xu X, Lei W, Zhang L (2006) Food Hydrocolloids 20:723
25. Cho J, Heuzey MC, Bégin A, Carreau PJ (2006) J Food Eng 74:500
26. Redgwell RJ, Schmitt C, Beaulieu M, Curti D (2005) Food Hydrocolloids 19:1005
27. Richardson PH, Willmer J, Foster TJ (1998) Food Hydrocolloids 12:339
28. Barré LL (2004) PhD Thesis. University of Southampton: Southampton, 2004
29. Olley RH, Hodge AM, Bassett DC (1979) J Polym Sci: Polym Phys Ed 17:627
30. Huggins ML (1938) J Phys Chem 42:911
31. Huggins ML (1939) J Phys Chem 43:439
32. Huggins ML (1942) J Am Chem Soc 64:2716
33. Kraemer EO (1938) Ind Eng Chem 30:1200
34. Flory PJ (1953) Principles of polymer chemistry. Cornell University Press, New York, p 310
35. Sudduth RD (1997) J Appl Polym Sci 66:2319
36. Hacche LS, Washington GE, Brant DA (1987) Macromolecules 20:2179
37. Casassa EF, Berry GC (1989) In: Booth C, Price C (eds) Comprehensive polymer science, vol. 2: Polymer properties. Pergammon Press, Oxford, p 71
38. Tayal A, Khan SA (2000) Macromolecules 33:9488
39. Bradley TD, Mitchell JR (1988) Carbohyd Polym 9:257
40. Hamley IW (2000) Introduction to soft matter. Wiley, Chichester
41. Barlow RJ (1989) Statistics. Wiley, Chichester
42. Goycoolea FM, Morris ER, Gidley MJ (1995) Carbohyd Polym 27:69
43. Azero EG, Andrade CT (2002) Polym Test 21:551
44. Gaisford SE, Harding SE, Mitchell JR, Bradley TD (1986) Carbohyd Polym 6:423
45. Pai VB, Khan SA (2002) Carbohyd Polym 49:207
46. Picout DR, Ross-Murphy SB, Errington N, Harding SE (2001) Biomacromolecules 2:1301
47. Zhbankov RG, Firsov SP, Buslov DK, Nikonenko NA, Marchewka MK, Ratajczak H (2002) J Molec Struct 614:117
48. Proniewicz LM, Paluszkiewicz C, Weselucha-Birczynska A, Baranski A, Dutka D (2002) J Molec Struct 614:345
49. Proniewicz LM, Paluszkiewicz C, Weselucha-Birczinska A, Majcherczjyk H, Baranski A, Konieczna A (2001) J Mol Struct 596:163
50. Kizil R, Irudayaraj J, Seetharaman K (2002) J Agric Food Chem 50:3912
51. Zhbankov RG, Firsov SP, Grinshpan DD, Baran J, Marchewka MK, Ratajczak H (2003) J Mol Struct 645:9
52. Mrozek MF, Weaver MJ (2002) Anal Chem 74:4069
53. Bell AF, Barron LD, Hecht L (1994) Carbohydr Res 257:11
54. Zhbankov RG, Firsov SP, Korolik EV, Petrov PT, Lapkovski MP, Tsarenkov VM, Marchewka MK, Ratajczak H (2000) J Mol Struct 555:85